

Journal of Materials Chemistry C

Accepted Manuscript



This is an *Accepted Manuscript*, which has been through the Royal Society of Chemistry peer review process and has been accepted for publication.

Accepted Manuscripts are published online shortly after acceptance, before technical editing, formatting and proof reading. Using this free service, authors can make their results available to the community, in citable form, before we publish the edited article. We will replace this *Accepted Manuscript* with the edited and formatted *Advance Article* as soon as it is available.

You can find more information about *Accepted Manuscripts* in the [Information for Authors](#).

Please note that technical editing may introduce minor changes to the text and/or graphics, which may alter content. The journal's standard [Terms & Conditions](#) and the [Ethical guidelines](#) still apply. In no event shall the Royal Society of Chemistry be held responsible for any errors or omissions in this *Accepted Manuscript* or any consequences arising from the use of any information it contains.

ARTICLE

Symmetric Naphthalenediimidequaterthiophenes for Electropolymerized Electrochromic Thin Films

Cite this: DOI: 10.1039/x0xx00000x

V. Figà,^a C. Chiappara,^a F. Ferrante,^a M. P. Casaletto,^b F. Principato,^a S. Cataldo,^a Z. Chen,^c H. Usta,^d A. Facchetti*^{c,e} and B. Pignataro*^aReceived 00th January 2012,
Accepted 00th January 2012

DOI: 10.1039/x0xx00000x

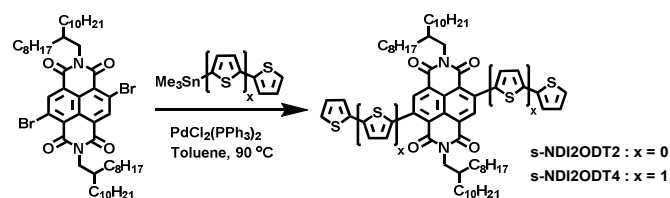
www.rsc.org/

A new symmetric naphthalenediimidequaterthiophene (s-NDI2ODT4) was synthesized and exhibited the capability to electropolymerize alone or with EDOT affording polymers with controlled donor/acceptor monomer ratios. s-NDI2ODT4-EDOT-based copolymers showed low band gaps, wide optical absorption ranges extending to the near IR region, tuned electrical properties, thin-film surface morphology and hydrophilicity as well as high coloration efficiency in electrochromic devices.

Introduction

Conjugated polymers endowed with electron-withdrawing and electron-donating moieties have attracted great interest because of their promising optical and electronic properties.¹ For this reason, several research groups have addressed their efforts towards the design engineering and synthesis of new push-pull systems to be used in organic opto-electronic devices. Several of these systems contain thiophene rings, such as alkyl- and alkoxy-oligothiophenes and ethylenedioxythiophene (EDOT), because of their strong electron-donor character.² Recently, perylenes and naphthalenes derivatives have been employed as electron-accepting moieties for realizing semiconducting small-molecules and polymers.³ Push-pull co-polymers comprising naphthalenediimide (acceptor) and thiophene (donor) derivatives have shown high air-stability, good processability, low band gap, and large electron mobilities,⁴ principally due to their substantial crystalline structure or ordered supramolecular packing.⁵ Several combinations of naphthalene derivatives and thiophene-based donor groups have been reported in the literature and their transport properties have been studied by several groups.⁶ Naphthalenediimide-based polymers have also been employed in different kind of devices. For instance, poly{[N,N'-bis(2-octyldodecyl)-naphthalene-1,4,5,8-bis(dicarboximide)-2,6-diyl]-alt-5,5'-(2,2'-bithiophene)} (P(NDI2OD-T2)) together with poly(3-hexylthiophene-2,5-diyl) (P3HT) have been employed in very high fill factor solar cells.⁷ P(NDI2OD-T2) and poly(N,N'-dialkylperylene-dicarboximide-dithiophene) (P(PDI2OD-T2)) have been used for fabricating bottom and top gate OTFT with mobilities up to 0.45-0.85 cm²/Vs,^{4b} and more recently

surpassing 2.5 cm²/Vs.⁸ P(NDI2OD-T2) allowed realizing monolayer polymeric field effect transistors^{9a} as well as vertical transistors.^{9b} Furthermore, molecules based on 1,4,5,8-naphthalenecarboxylic-diimide with thiophenes substituents have been studied and the effect of the number of thiophene moieties between two naphthalene unities on the polymeric optic and electronic properties have been investigated.⁹ More recently, the polymer P(NDI-TVTV) showed field-effect electron mobilities as high as 1.5 - 1.8 cm²/Vs.¹⁰



Scheme 1. Chemical structure and synthesis of s-NDI2ODT2 and s-NDI2ODT4.

On the other hand, the combination of the strong electron-donor and self-structuring effects of EDOT with electron accepting systems has been employed as a powerful tool for the design and synthesis of π -conjugated copolymers with a diverse range of optical and electro-optical properties.¹¹ Thus, associating EDOT with strong electron-withdrawing building blocks enabled rigidified π -structures with improved planarity and greatly reduced band gaps.¹² For instance, copolymers achieved by polymerization of EDOT with electron acceptor units such as cyanovinylene, thieno[3,4-b]pyrazine or benzo[1,2-c:4,5-c']bis[1,2,5]thiadiazole enabled bandgaps from ~1.50 eV to as low as ~0.40 eV.¹² Interestingly, systems

bearing EDOT have been employed to synthesize copolymers with electrochromic behaviour extending in the IR region.¹³ However, very few works have investigated the electrochromic properties of naphthalenediimide-based polymers, the most promising achieving polymers with good stability, high transmissivity and high coloration efficiency.¹⁴ Interestingly, both naphthalenediimide with thiophene substituents and EDOT¹⁵ displayed low oxidation onset potentials which allows their electrochemical polymerization in common organic solvents.

In this work, we designed and synthesized two novel symmetric naphthalenediimidethiophenes, namely *N,N'*-bis(2-octyldodecyl)-2,6-bis(2-thienyl)naphthalene-1,4,5,8-bis(dicarboximide) (*s*-NDI2ODT2) and *N,N'*-bis(2-octyldodecyl)-2,6-bis(5-(thioph-2-yl)thiophen-2-yl)naphthalene-1,4,5,8-bis(dicarboximide) (*s*-NDI2ODT4) (Scheme 1). Their symmetric structure has been designed to allow for regioregular electropolymerization with EDOT. For *s*-NDI2ODT4, electropolymerized films with new structural and optoelectronic properties along with electrochromic devices are achieved and discussed.

Results and Discussion

Monomer Synthesis and Characterization

The synthesis of *s*-NDI2ODT2 and *s*-NDI2ODT4 was carried out under argon by reacting a mixture of 2-(trimethylstannyl)thiophene and 5-(trimethylstannyl)-2,2'-dithiophene, respectively, with NDI2OD-Br₂ and Pd(PPh₃)₂Cl₂ in anhydrous toluene. Upon cooling to room temperature, the reaction mixtures have been diluted with chloroform and then washed with water, dried over anhydrous sodium sulfate, and concentrated on rotary evaporator. The residues were subjected to column chromatography on silica gel with a mixture of chloroform:hexane as eluent, leading to an orange (*s*-NDI2ODT2) or a purple (*s*-NDI2ODT4) solid as the product (Scheme 1). Synthetic and characterization details can be found in the ESI. From optical absorption spectroscopy in acetonitrile:dichloromethane solution (2:3; v:v), the maximum absorption for *s*-NDI2ODT2 and *s*-NDI2ODT4 are located at 250 nm and 300 nm, respectively. Cyclic voltammetry (CV) measurements carried out in acetonitrile:dichloromethane solution (2:3; v:v) containing 10⁻² M of LiClO₄ and 10⁻⁴ M of the monomers indicate oxidation onset potentials located at +1.6V and +1.15V for *s*-NDI2ODT2 and *s*-NDI2ODT4, respectively and oxidation peaks located at +1.8V and +1.24 V, for *s*-NDI2ODT2 and *s*-NDI2ODT4 respectively. Reversible oxidations have not been observed, however, the onset of these processes are shifted to more positive potentials for *s*-NDI2ODT2 versus *s*-NDI2ODT4. This result corroborate that the presence of a greater number of electron-rich thiophene units facilitate oxidation.

Electropolymerization

We performed electrochemical polymerizations of the pristine NDI-based monomers alone and in the presence of EDOT to modulate the polymer properties. Our results show that while *s*-NDI2ODT2 did not electropolymerize under several conditions, *s*-NDI2ODT4 alone or in the presence of EDOT showed the efficient formation of solid thin films supported on the electrode. These results can be rationalized by the deactivation of the thiophene pendant radical cation of *s*-NDI2ODT2 due to the contiguity of the strongly electron-accepting NDI moiety. Deactivation of electropolymerization in electron-depleted moieties have been reported for other classes of compounds.¹⁶ On the other hand, in *s*-NDI2ODT4 the external thiophenes may be easily polymerize since they are spaced from the NDI unit by the internal thiophene. Thus, the new compound *s*-NDI2ODT4 represents a new entry to achieve electropolymerize NDI2OD-oligothiophene-based systems. Electropolymerized PNDI2ODT4, PEDOT and (NDI2ODT4)_m-(EDOT)_n copolymers with different ratios were obtained by CV (Ag/AgCl, 3.5 M KCl). For all the systems, the electrode potential has been increased from the open circuit value to +1.3V and reversed to the open circuit value for several cycles.

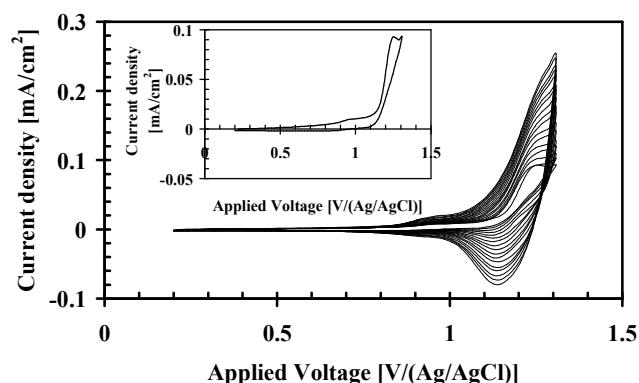


Figure 1. Cyclic voltammetry of a 10⁻⁴ M acetonitrile:dichloromethane solution (2:3; v:v) of *s*-NDI2ODT4 containing 10⁻² M of LiClO₄, recorded using glassy carbon (S=0.07 cm²) as working electrode. Inset: First cycle of the CV plot.

Figure 1 displays CV scans for *s*-NDI2ODT4 in acetonitrile:dichloromethane solution (2:3; v:v) containing 10⁻² M of LiClO₄ and 10⁻⁴ M of the monomer at a potential scan rate of 50 mV/s. The first cycle presents an oxidation potential onset of +1.15 V that indicates the potential at which the monomer starts to be oxidized. The current reaches a peak value at +1.24 V. The oxidation onset lowered with the number of cycles suggesting that the previously formed oligomers are easier to oxidize than the monomer. As the CV scan continues, the polymer film is formed at the working electrode. The film thickness increases with the number

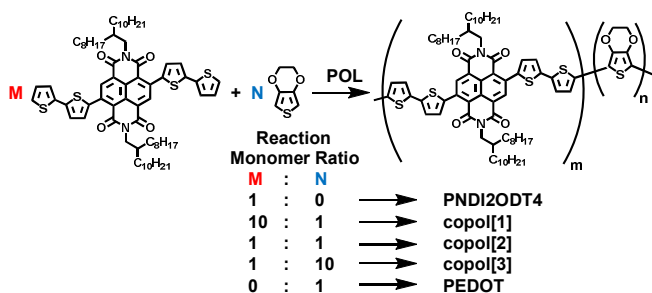


Figure 2. Chemical structure of the NDI2ODT4:EDOT electropolymerized copolymers with M and N indicating the monomer loading ratios and m and n the number of incorporated NDI2ODT4 and EDOT units in the structure, respectively.

of CV cycles as suggested by the current rising. CV curve shapes differ when going from the polymerization of NDI2ODT4 or EDOT to that of $(\text{NDI2ODT4})_m\text{-(EDOT)}_n$, suggesting successful copolymerizations and incorporation of both monomers. Three s-NDI2ODT4:EDOT molar ratios have been used affording the following copolymers: copol[1] (10:1), copol[2] (1:1), copol[3] (1:10) (Figure 2).

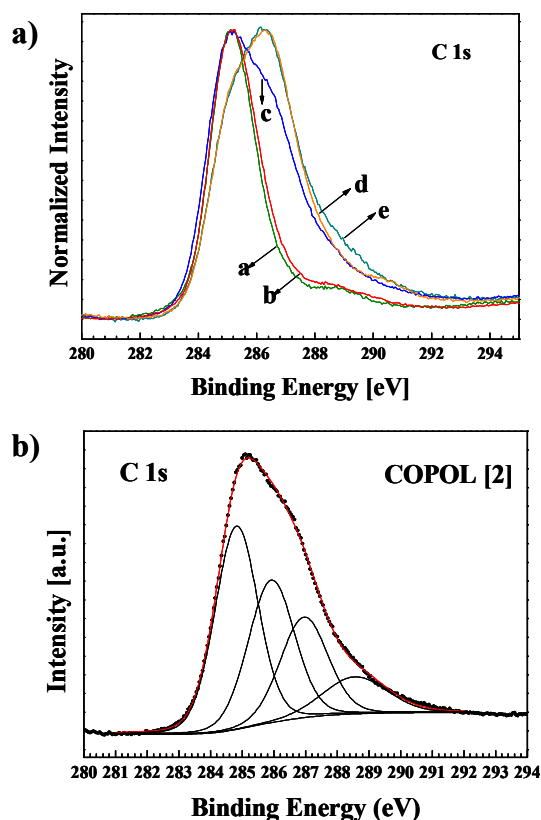


Figure 3. a) Normalized C1s XPS spectra of the electropolymerized thin films: a) PNDI2ODT4; b) PEDOT; c) copol [2]; d) copol [1] and e) copol [3], all electrodeposited onto ITO/PET substrates. b) XPS curve-fitting of the C 1s photoelectron spectrum of the Copol [2] thin film.

Both homopolymer and copolymer thin films were chemically characterized by XPS analysis (Fig. 3). As expected, the oxygen, carbon, nitrogen and sulphur elements are present in all the thin films wide spectra. Figure 3a shows the XPS C1s spectra of the different electropolymerized thin films. The C1s peak shape of the copol[1] and copol[3] copolymers closely resemble those of predominant PNDI2ODT4 and PEDOT, respectively. The C1s peak of copol[2] copolymer appears quite different being located in-between the two homopolymers. As resulted from the curve-fitting procedure, the XPS C1s spectrum of copol[2] can be deconvoluted by four components, as reported in Figure 3b. The component located at a binding energy (B.E.) of 284.5 eV is assigned to C-C, C=C, C-H bonds; the component at B.E.=285.9 eV is attributed to C-S, C-N bonds; the component located at B.E.=286.7 eV corresponds to the presence of C-O bonds and the component at B.E.= 288.3 eV is typical of N-C=O bonds.³¹ Results of the XPS C1s curve-fittings of the other samples are reported in the ESI. By considering the surface C/S atomic percentage ratios (see Table 1) and the C_{1s} deconvoluted peaks (see ESI), it is possible to establish the actual monomer incorporation in the $(\text{NDI2ODT4})_m\text{-(EDOT)}_n$ copolymers as a function of the monomer concentration ratios employed for the electropolymerization (Fig. 2). Thus, in addition to the

Table 1. XPS surface chemical quantitative analysis of the electropolymerized thin films. Elemental composition is expressed as atomic percentage.^a

SAMPLE	C 1s	O 1s	N 1s	S 2p	In 3d	Sn 3d
PNDI2ODT4	70.5	18.4	2.0	3.1	5.3	0.7
COPOL [1]	81.9	11.0	1.9	4.7	0.4	---
COPOL [2]	67.3	23.4	1.4	7.1	0.7	---
COPOL [3]	68.6	23.8	0.8	6.5	0.3	---
PEDOT	58.4	33.4		7.8	0.4	---

^aIn3d and Sn3d photoelectron signals originate from the ITO substrate. No ClO⁺ doping anions have been observed by XPS in these samples.

PNDI2ODT4 and PEDOT homopolymers, we reasonably formed $(\text{NDI2ODT4})_m\text{-(EDOT)}_n$ copolymers with $4 < m < 8$ and $n=1$ in the case of copol[1], $m=1$ and $4 < n < 5$ for copol[2], and $m=1$ and $n=8$ for copol[3]. XPS shows that the increasing in EDOT content leads to a higher surface oxygen content, which should indicate a more hydrophilic film as also observed by water contact angle experiments. Water contact angle ranges from 107.7° for PNDI2ODT4 to about 65.35° for copol[3] (see ESI).

Polymer Electronic Structure

In order to investigate the nature of the electronic transitions, molecular models of NDI2ODT4-(EDOT)_n-

NDI2ODT4, ($n = 0, 1, 4$), (EDOT) $_n$ ($n = 8, 12, 16$) and (EDOT) $_n$ -NDI2ODT4-(EDOT) $_n$ ($n = 3-8$) systems were subjected to full geometry optimization and subsequent TDDFT calculations. The computed molecular geometries are qualitatively similar to those reported for analogous species, such as the P(NDI2OD-T*) series^{6,17}: the NDI moiety and the bonded thiophene-derivative chain lie in planes tilted by approximately 50°, and this strongly reduces electron conjugation throughout the polymer chain. The results obtained for the first three singlet-singlet vertical transitions are reported in Table S1 of the ESI together with their oscillator strengths. The transition at lower energy in the investigated structures has a charge-transfer (CT) nature, with electron density migrating from the π -system of the EDOT chain to the π -system of NDI2ODT4. The HOMO and the LUMO are the molecular orbitals most largely involved in this CT transition, but in the larger systems several other quasi-degenerate orbitals can be observed with sensible weights. In particular, while the inclusion of one EDOT between two NDI2ODT4 units leads to a slight energy decrease of the $S_0 \rightarrow S_1$ CT transition, in NDI2ODT4-(EDOT) $_4$ -NDI2ODT4 the appearance of a second intense transition ($S_0 \rightarrow S_3$) can be noted, involving the EDOT π -system. The $S_0 \rightarrow S_2$ transition is forbidden or very weak in the oligomers. Thus, in the NDI2ODT4-(EDOT) $_n$ -NDI2ODT4 series, the $S_0 \rightarrow S_1$ transitions are found at

absorption spectra of: PNDI2ODT4 (a), copol [1] (b), copol [2] (c), copol [3] (d) and PEDOT (e).

2.472, 2.385, 2.225 eV for $n = 0, 1, 4$, respectively. In the same way, the insertion of one NDI2ODT4 unit into EDOT for the (EDOT) $_n$ -NDI2ODT4-(EDOT) $_n$ ($n = 3-8$) series causes the occurrence of a CT transition at energy (from 2.212 eV for $n = 3$ to 2.151 eV for $n = 8$) lower than the $\pi \rightarrow \pi^*$ transition (from 2.821 eV for $n = 3$ to 2.520 eV for $n = 8$). In other words, when the orbital conjugation in PEDOT is interrupted by NDI2ODT4 units, the CT transition shifts to higher wavelength (fig. 4a). So, this transition energy could be modulated by the appropriate choice of the NDI2ODT4-EDOT ratio in the copolymer. Finally by comparing the HOMO and LUMO representations of the EDOT-NDI2ODT4-EDOT molecule, a different phase is observed in one of the linkage points (see ESI). Accordingly, this result would suggest that the polymer is a direct gap semiconductor¹⁸.

Fig. 4b displays the UV-Vis absorption spectra of PNDI2ODT4 and PEDOT homopolymers together with those of the copol[1], copol[2] and copol[3]. The convolution of the PEDOT and PNDI2ODT4 spectra does not show the same peak shapes observed for the copolymers as a further proof of the successful copolymerization process. In particular, the spectra of PNDI2ODT4 displays two transition bands: the high energy band (350-450 nm) may be attributed to excited states more localized on thiophene units ($\pi \rightarrow \pi^*$ transition), whereas the low energy band (550-800 nm) can be assigned to an intramolecular charge transfer transition.⁶ Electropolymerized PEDOT shows just a broad absorption band at long wavelengths typical of the oxidized form.¹⁹ In addition to the NDI2ODT4 $\pi \rightarrow \pi^*$ and CT transition bands, copol[2] presents a shoulder in the 440-500 nm region that can be ascribed to new components typical of the copolymer system. This shoulder increases with the EDOT amount. By considering the PNDI2ODT4 homopolymer and copol[2], it is possible to observe a red shift of the CT transition band as well as a spectral absorption up to the near IR region as an indication that by adding EDOT units to NDI2ODT4 a band gap reduction occurs. A red shift in the CT transition band cannot be otherwise observed for further increased amount of EDOT because of the overlapping of the broad absorption band at long wavelengths. Interestingly, by opportunely modulating the monomers ratio (see for instance copol[2]) it is possible to obtain copolymers with a wide optical absorption range with a solar spectrum coverage including both visible components and the near IR region as confirmed by spectroscopic investigation up to about 1020 nm.

The optical band gap has been calculated under the above hypothesis of direct optical transitions,²⁰ by plotting $(\alpha h\nu)^2$ vs $h\nu$, fitting the straight portion and

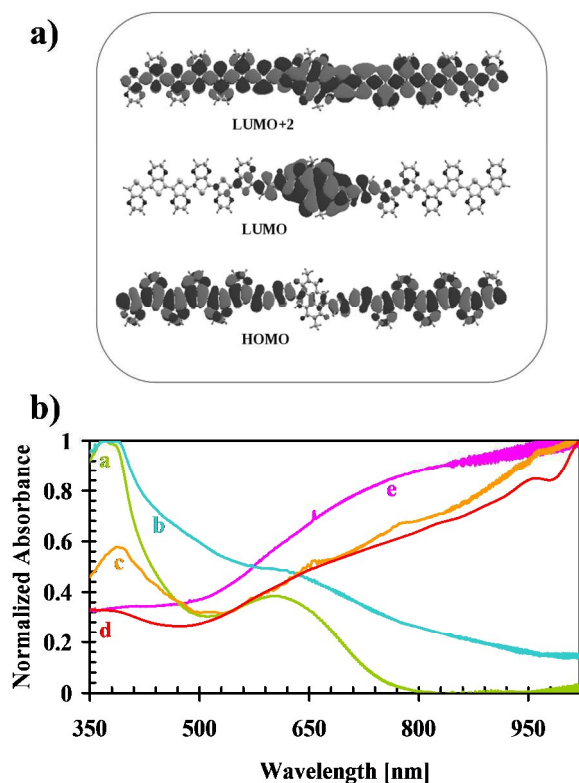


Figure 4. a) DFT computations of (EDOT) $_6$ -NDI2ODT4-(EDOT) $_6$ showing selected MO topologies. b) Optical

extrapolating to $(\alpha h\nu)^2=0$. In particular, by increasing the EDOT content in the copolymer systems, we notice a decreasing of the optical band gap spanning from 1.5 eV to 1.15 eV for copol[1] and copol[2], respectively (see ESI). This trend is consistent with the DFT calculations reported above and the literature results for EDOT-NDI copolymers.²¹ This result suggests that by the NDI2ODT4-EDOT copolymerization we can design copolymers with appropriate optical properties including band gap modulation and controlled optical absorption in the near UV and near IR regions.

Polymer Film Morphology and Charge Transport

Figure 5 shows scanning electron microscopy (SEM) images for selected electropolymerized films, highlighting the morphological changes upon EDOT incorporation. Thus, PNDI2ODT4 film is quite compact

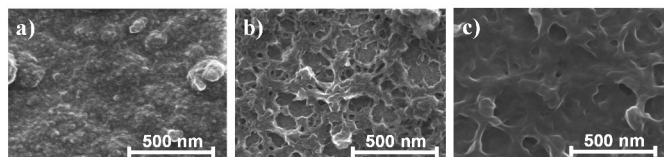


Figure 5. SEM images of PNDI2ODT4 (a), copol[2] (b), PEDOT (c).

with a surface morphology characterized by particle grain size of 8–20 nm, whereas copol[1] displays a globular structure with 10–40 nm size particles. By increasing the EDOT amount, copol[2] film is mainly porous with features spanning 10–180 nm. Copol[3] displays a mixed morphology with reduced porous features (15–100 nm large) together with globular nanoparticles of 10–90 nm in size. Finally, PEDOT thin films show branched features with the presence of few pores with a diameter of 30–250 nm (for further morphological details see ESI). The data shown above indicates that the incorporation of EDOT into NDI2ODT4 gives rise to branched thin film supramolecular structures with the formation of porous features. For a number of applications, it may be desirable to achieve more smooth film surfaces. By thermally annealing the thin films at about 160 °C for 40 minutes a surface smoothing has been obtained (see ESI, fig. S9b about 20% decrease in roughness of copol[2] by AFM).

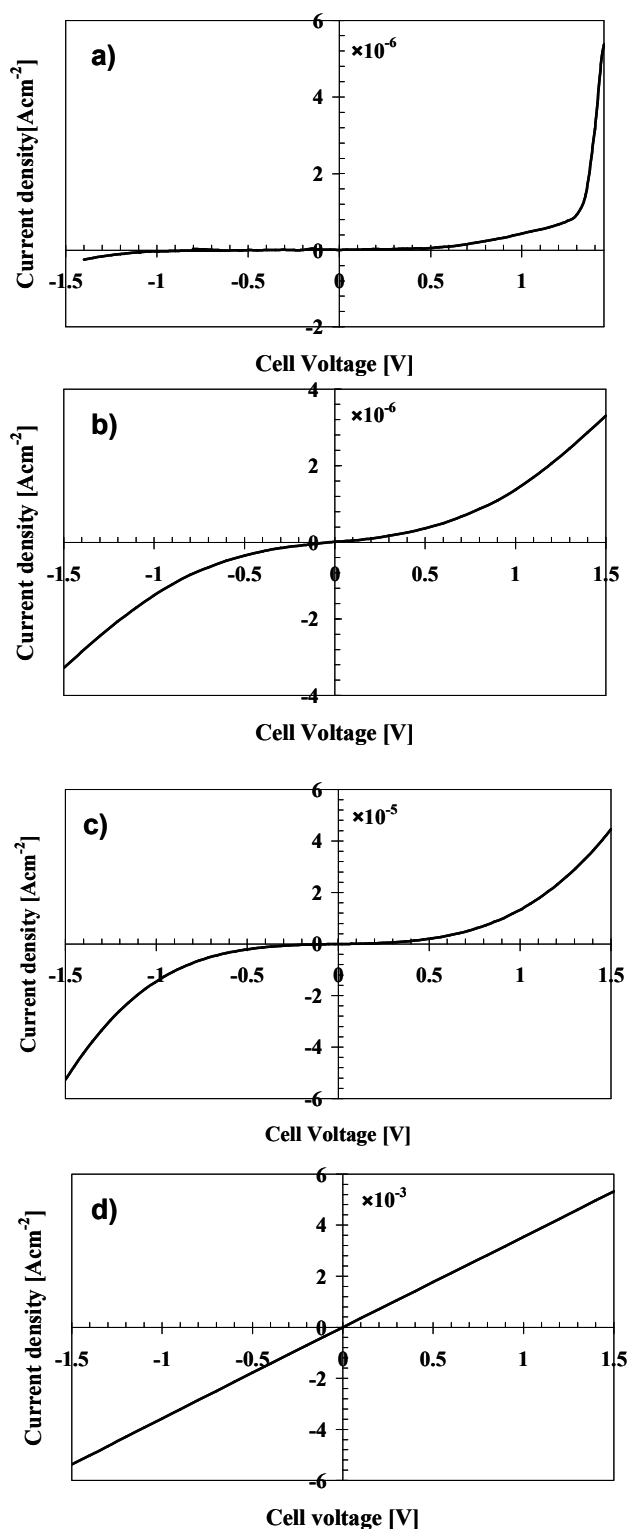


Figure 6. Current density-voltage plots for PNDI2ODT4 (a), copol[1] (b), copol[2] (c), PEDOT (d).

Charge transport measurements on the electropolymerized films (400–500 nm thick) using a mercury probe indicate a progressive trend from a

rectifying behavior for PNDI2ODT4 to the degenerate semiconducting behavior for PEDOT. In particular, whereas electrodeposited PEDOT gives an ohmic behavior with conductivity of about 6 S/cm,²² copol[2] leads to an ohmic behavior (conductivity of about 10⁻⁵ S/cm) at low bias potential and to a space charge limited current (SCLC) regime at higher bias obeying to a I=KV² law. A similar behavior is observed for copol[1] but with conductivity in the order of 10⁻⁶ S/cm, whereas PNDI2ODT4 shows a threshold potential of about 1.4 V (Fig. 6; see ESI for further details). From Equation [1]²³

$$J_{SCL} = \frac{9}{8} \epsilon_0 \epsilon_r \mu \frac{V^2}{d^3} \quad \text{Eq. [1]}$$

which governs the transport in a space-charge limited current regime, (where J_{SCL} = space charge limited current; V=voltage; d=thickness, μ =charge carriers mobility, ϵ_0 =permittivity in vacuum, ϵ_r =relative static permittivity), the carrier mobility values of copol[1] and copol[2] were found to be 2.5×10⁻⁷ cm²/Vs and 1.7×10⁻⁶ cm²/Vs, respectively, using SCLC measurements. These results suggest that by increasing the EDOT moiety content, the copolymers exhibit higher carrier mobilities in agreement with the greater content of the electron-rich EDOT.

Optoelectronic Properties

From cyclic voltammetric experiments, we have found that the onset oxidation potential of EDOT rich copol[2] and copol[3] polymers is ~1.5 V and it is larger than that of both PEDOT (0.95 V) and PNDI2ODT4 (1.15 V). This result indicates that copolymer-based thin films are more stable toward electrochemical oxidation than the respective homopolymers due to a strong coupling between the two different donor-acceptor monomer units. This effect has been observed for some thiophene-based copolymer classes and monomer mixtures.²⁴ The optoelectronic properties of homopolymers and copolymers thin films were investigated for understanding the changes in transmittance due to different redox states. For this reason, films of about 200 nm were electrodeposited onto transparent ITO/PET electrodes (2.4 cm²). The characterization was led by employing 0.1 M LiClO₄ in CH₃CN and by using a two-electrodes configuration in a 1 cm path length cuvette endowed with quartz windows. For the estimation of the optical contrast and response time, we applied square wave potentials (SWP) and transmittance vs time curves were recorded at suitable wavelengths (λ). The best conditions (potential and λ) were identified by recording the absorption spectra of the films at different polarization potentials.

Table 2. Summary of the electrochemical and optical data for the different electropolymerized thin films.^a

POLYMER	Oxidation onset [V/(Ag/AgCl)]	λ_{max} [nm]	$E_{g,opt}$ [eV]	Response time [sec]	ΔT [%] at $\pm 1.5V$
PNDI2ODT4	1.15	370	1.71	108 o→r 250 r→o	*19
copol[1]	1.15	370	1.50	50 o→r 20 r→o	*20
copol[2]	1.50	390	1.15	13 o→r 15 r→o	37
copol[3]	1.50	N.D.	N.D.	10 o→r 13 r→o	30
PEDOT	0.95	N.D.	N.D.	12 o→r 10 r→o	34

^a For copol[3] and PEDOT it was not possible to determine precise λ_{max} and optical band gap ($E_{g,opt}$) values (see ESI). * For PNDI2ODT4 and copol[1], $\Delta T\%$ has been evaluated by applying $\pm 0.8V$.

The PNDI2ODT4 polymer displays the highest optical contrast of 19% between +0.8V and -0.8V and at 900 nm (Figure 7a); furthermore it displays high stability in the explored time and potential ranges. It appears green and light brown in the oxidized (+0.8V) and reduced (-0.8V) states, respectively. Note, this polymer is also green in the neutral state. By considering the electrochemical charge required for a complete switching and the optical density at 900 nm, a coloration efficiency of 302 cm²C⁻¹ were calculated. This value is comparable with the coloration efficiency of novel classes of poly(ether-imide)s.²⁵ PNDI2ODT4 exhibits slow response times compared to other poly(naphthalene)s derivatives.²⁶ Thus, it requires 110 seconds for shifting from the oxidized to the reduced state and 250 seconds for the inverse process, suggesting different charge transfer kinetics for the oxidized and reduced PNDI2ODT4 species. The presence of EDOT moieties in the NDI2ODT4 based chain improves the electrochromic response of the resulting copolymers in terms of both optical contrast and response time. Thus, copol[2] exhibits an optical contrast up to 37% at 580 nm and response times of 13 (ox→red) and 15 (red→ox) seconds (Figure 7b) under a square wave potential between +1.5V and -1.5V. By increasing the EDOT amount, as it is in the case of copol[3], the optical contrast saturates to similar values but at 588 nm. This shift could be attributed to the greater EDOT content since PEDOT highest optical contrast is recorded at ~600 nm.²⁸ Also, these values are ~10 % higher than those measured for different electrochemically synthesized EDOT-naphthalene based copolymers, which have displayed an optical contrast of 26%.²⁹ Copol[1] exhibited the same optical contrast of PNDI2ODT4 at 900 nm and shorter response times but it has appeared unstable (see ESI). Table 2 shows the performance parameters for the different electropolymerized systems.

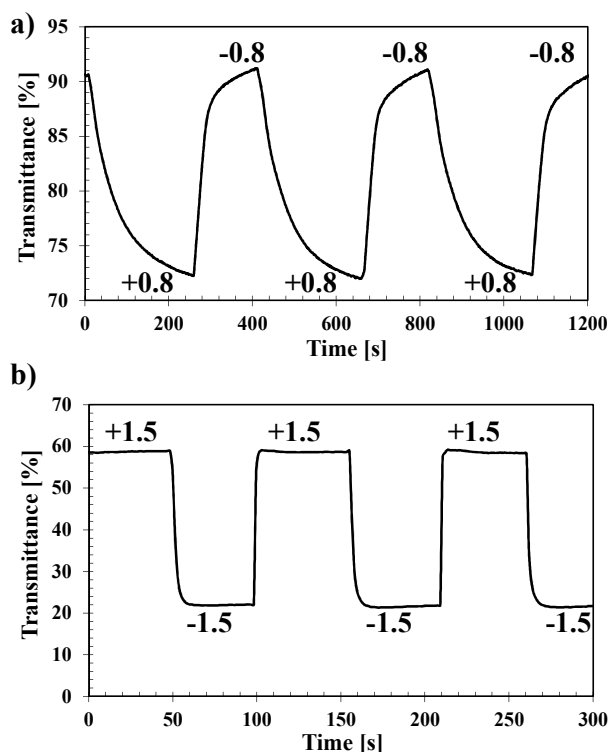


Figure 7. Transmittance vs time plots in CH_3CN (0.1 M LiClO_4) for: a) PNDI2ODT4 thin films at 900 nm and b) copol[2] thin films at 580 nm.

Clearly, the optical contrast and the response time depends of the co-polymer chemical composition, thus giving a range of possible applications for these systems. In particular, while the response time and transmittance values of PNDI2ODT4 may be of interest for smart windows or optical filters,²⁷ the lower response time and higher optical contrast of copol [2] and copol [3] is interesting for simple passive matrix displays.²⁷

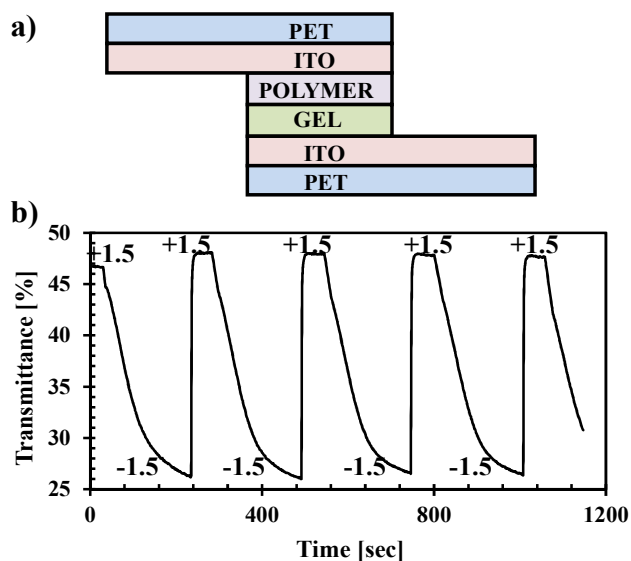


Figure 8. a) Solid state ECD configuration and b) transmittance vs time plots of a representative copol[2]-based ECD.

The copolymers with the best electrochromic performances were employed for the fabrication of solid state electrochromic devices (ECD). Thus, copol[2] and copol[3] electrodeposited onto ITO/PET electrodes were sandwiched with a second ITO/PET electrode using a polymethylmethacrylate (PMMA)-based gel electrolyte (Fig. 8a). These devices were subjected to a square wave potential between $\pm 1.5\text{V}$ and the transmittance vs time plots have been recorded by irradiating at 580 nm and 588 nm, respectively. The potential range from $+1.5\text{V}$ to -1.5V was used since it enables the highest switching rate and the maximum optical contrast along with stability.

In particular, copol[2] (fig. 8b) and copol[3] based ECDs showed an optical contrasts of 22% and 29%, respectively. The response times of these devices are about 15 seconds from reduced to oxidized states. In figure 8b (as for 7a) the potential switching from the oxidized to the reduced states occurs in about 200 sec without reaching a complete saturation, which requires a longer time but with negligible ($<3\%$) ΔT gain. The stability of copol[2] and copol[3] based ECD was evaluated by measuring the optical change in the time domain at 580 nm and 588 nm, respectively. As reported in fig. 8b preliminary data suggest stability for copol[2], the optical contrast being constant in time as it maintains the same value of transmittance under the applied voltages. Copol[3] based ECDs showed reduced stability with respect to those with Copol[2] as indicated in Fig. S13b. The substantial stability of copol [2] based ECDs in the explored time ranges, suggests that they are promising materials for different electrochromic applications.

Conclusions

In conclusion, we have identified the s-NDI2ODT4 monomer as a very attractive systems for developing new electropolymerized naphthalenediimide-based copolymers with EDOT having controlled monomer ratios. This approach allows copolymers with a modulation of fundamental properties including oxidation onset, band gap, optical absorption, carriers mobility, surface hydrophilicity, and film morphology. Among the NDI derivatives investigated to date, these systems exhibit very low band gap, wide optical absorption range with solar spectrum coverage up to the near IR region, and high coloration efficiency. Furthermore, we developed interesting electrochromic devices with tuned response time and optical contrast. The physical properties of s-NDI2ODT4 based copolymers might be of interest for other applications including photovoltaics, sensors and biosensors.

Experimental

Synthesis of Symmetric NDIT Systems

Preparation of N,N'-bis(2-octyldodecyl)-2,6-bis(2-thienyl)naphthalene-1,4,5,8-bis(dicarboximide) (NDI2OD-T1). Under argon, a mixture of NDI2OD-Br2 (280.0 mg, 0.28 mmol), 2-trimethylstannylthiophene (400.0 mg, 1.62 mmol), Pd(PPh₃)₂Cl₂ (28.0 mg, 0.04 mmol) in anhydrous toluene (20 mL) was stirred at 90 °C for 22 h. Upon cooling to room temperature, the reaction mixture was diluted with chloroform (100 mL), and the resulting mixture was washed with water (80 mL), dried over anhydrous sodium sulfate (Na₂SO₄), and concentrated on rotary evaporator. The residue was subject to column chromatography on silica gel with a mixture of chloroform:hexane (3:2, v/v) as eluent, leading to an orange solid as the product (240.0 mg, 85.2%). ¹H NMR (CDCl₃ 500 MHz): δ : 8.77 (s, 2H), 7.57 (d, J = 5.0 Hz, 2H), 7.31 (d, J = 3.5 Hz, 2H), 7.21 (m, 2H), 4.07 (d, J = 7.5 Hz, 4H), 1.95 (m, 2H), 1.18-1.40 (m, br, 64H), 0.84-0.88 (m, 12H).

Preparation of N,N'-bis(2-octyldodecyl)-2,6-bis(5-(thiophen-2-yl)thiophen-2-yl)naphthalene-1,4,5,8-bis(dicarboximide) (NDI2OD-T2). Under argon, a mixture of NDI2OD-Br2 (1.00 g, 1.02 mmol), 5-(trimethylstannyl)-2,2'-dithienyl (1.34 g, 4.07 mmol), Pd(PPh₃)₂Cl₂ (0.095 g, 0.14 mmol) in anhydrous toluene (60 mL) was stirred at 90 °C for 16 h. Upon cooling to room temperature, the reaction mixture was diluted with chloroform (100 mL), and the resulting mixture was washed with water (100 mL), dried over anhydrous sodium sulfate (Na₂SO₄), and concentrated on rotary evaporator. The residue was subject to column chromatography on silica gel with a mixture of chloroform:hexane (3:2, v/v) as eluent, leading to a purple solid as the product (0.85 g, 72.0%). ¹H NMR (CDCl₂CDCl₂, 400 MHz): δ : 8.77 (s, 2H), 7.27-7.36 (m, 8H), 7.10 (dd, J = 4.8 Hz, J = 3.6 Hz, 2H), 4.09 (d, J = 7.2 Hz, 4H), 1.98 (m, 2H), 1.16-1.45 (m, br, 64H), 0.80-0.90 (m, 12H).

Electrochemical Thin Films Deposition

Electrochemical depositions of PNDI2ODT4, PEDOT and NDI2ODT4:EDOT copolymers have been performed by anodic oxidation of the monomers in a conventional three electrodes cell connected with a Potentiostat/Galvanostat (Metrohm Autolab PGSTAT 128N). No cathodic processes have been observed for these systems. This is not surprising since thiophene derivatives have been usually observed to polymerize anodically.³⁸ Thin films have been prepared potentiodynamically by sweeping the applied potential in a range between the open circuit value and +1.3V vs. Ag/AgCl, KCl (3.5M) for 17 cycles at a scan rate of 50 mV/s. They have been deposited on both glassy carbon (GC, diameter = 3 mm, Bio-Logic SAS) and ITO/PET (35 Ω /cm², Sigma Aldrich) with different active areas. A graphite wire has been used as counter electrode. Before each experiment, GC underwent a fine polishing procedure with 0.05 μ m white alumina suspension in a polishing pad, followed by ultrasonication in de-ionized water and acetone respectively. ITO/PET electrodes have been cleaned in acetone using an ultrasonic bath. The electrodeposition solution has been 10⁻² M of lithium perchlorate (LiClO₄ purum \geq 98%, Sigma Aldrich) in a mixture of acetonitrile (CH₃CN, anhydrous 99.8%, Sigma Aldrich) and dichloromethane (CH₂Cl₂, Chromasolv HPLC \geq 99.8%, Sigma Aldrich) (2:3; v:v) containing a monomer concentration of 10⁻⁴ M and different molar ratio in the case of copolymers. All the experiments have been performed at room temperature. After the thin films electrodeposition, the modified working electrodes have been washed with CH₃CN and CH₂Cl₂ mixture in order to remove the excess of both supporting electrolyte and monomers. The thin films thickness was estimated by the Faraday's law and confirmed by measurements with a 3D Optical Profiler (Sensofar).

X-ray photoelectron spectroscopy (XPS)

Photoemission spectra were collected by a VG Microtech ESCA 3000 Multilab spectrometer, equipped with a standard Al K α excitation source (h ν = 1486.6 eV) and a nine-channeltrons detection system. The hemispherical analyser operated in the CAE mode at a constant pass energy of 20 eV. The binding energy (BE) scale was calibrated by using C 1s peak (BE = 285.1 eV) from the adventitious carbon and the accuracy of the measure was \pm 0.1 eV. The ultrahigh vacuum (UHV) analysis chamber was evacuated to a pressure value lower than 1 x 10⁻⁶ Pa during data collection. Photoemission data were collected and processed by using the VGX900 software. Data analysis was performed by a nonlinear least square curve-fitting program using a properly weighted sum of Lorentzian and Gaussian component curves and peak area determination after background subtraction according to Shirley and Sherwood procedures.³⁵ The surface chemical composition of the investigated samples was obtained by using the sensitivity factor approach,³⁶ based on peak area intensities calculated by a standard quantification routine, including Wagner's energy dependence of attenuation length,³⁷ and a

standard set of VG Escalab sensitivity factors. The uncertainty on the atomic quantitative analysis is about $\pm 10\%$.

Computational Details

The structural and electronic properties of all systems studied computationally in this work has been performed by means of Density Functional Theory applying the oligomeric approach on model where the computationally cumbersome alkyl chains of the NDI2ODT4 moiety have been substituted by methyl groups. The singlet-singlet adiabatic electronic transitions have been investigated by means of the time dependent density functional approach (TDDFT) by using the Coulomb-Attenuating Method applied to the B3LYP exchange-correlation functional (CAM-B3LYP)³³ joined with the correlation consistent polarized valence double zeta basis set (cc-pvzd) basis set. The calculation has been performed on the electronic ground state geometries, fully optimized at the same level of theory. The CAM-B3LYP functional revealed to be a reliable choice for the calculation of singlet-singlet electronic transition energies in organic molecules³¹ and particularly for the case of charge-transfer transitions³². All calculation have been performed by employing the Gaussian 09 package.³³

Thin Film Characterization

Electrochemical behaviour of electrodeposited PNDI2ODT4, PEDOT and NDI2ODT4:EDOT copolymer deposited on GC electrodes has been studied by means of cyclic voltammetry (CV) in CH₃CN containing 0.1M LiClO₄ as supporting electrolyte at room temperature. Morphological investigations about the surface have been carried out by using both Scanning Electron Microscopy (SEM). SEM studies have been performed using a FEI FEG-ESEM (mod. QUANTA 200) at different voltages and magnifications. Gold has been sputtered onto the samples before the morphological analysis. Absorption spectra were recorded using a Beckman DU-640 spectrophotometer equipped with a 150 W xenon arc lamp as excitation source. Spectroelectrochemical measurements have been performed by coupling both the Beckman DU-640 spectrophotometer and the Metrohm Potentiostat/Galvanostat. Two electrodes cell configuration has been used for this purpose. Transmittance vs time plots under the applied square wave potential were recorded at the optimized wavelengths of 900 nm for PNDI2ODT4 and copol[1], 580 nm for copol[2], 588 nm for copol[3], and 600 nm for PEDOT. The response times have been calculated for about 100% of colour changes. The electrical measurements have been performed by a Keithley 4200-SCS Parameter Analyzer, configured in the voltage sweep mode. The metal contact with the organic thin layers electrodeposited on ITO/PET substrate was realized with circular orifices through Polytetrafluoroethylene (PTFE) substrate filled with mercury (Hg). The Hg contact area was 0.05 cm². The voltage has been maintained positive whereas the Hg potential was higher than that of ITO.

AFM Analysis

The surface morphology has been investigated by using an AFM Nanoscope V (Veeco Instruments Inc., Santa Barbara, California). Images (512x512 points, 1 Hz scan rate) have been acquired in dynamic-contact mode (TappingMode) by using silicon probes (RTESP-type, Veeco) with a nominal tip curvature of 10 nm.

Electrochromic Device Construction

Solid state electrochromic devices have been fabricated in a common sandwich configuration. NDI2ODT4:EDOT copolymers thin films electrodeposited on ITO/PET have been separated from ITO/PET counter electrodes by means of a transparent gel electrolyte. LiClO₄ (0.3 g) and poly(methyl methacrylate) (PMMA; Mw:120,000 Sigma Aldrich) (0.7 g) have been dissolved in acetonitrile (7 g) and propylene carbonate (2 g) has been added as plasticizer. The obtained gel electrolyte has been spread onto the polymeric film and finally the counter electrode has been added on the top.

Acknowledgements

Italian MiUR is acknowledged for funding through FIRB - Futuro in Ricerca (RBF08DUX6) and PON R&C 2007– 2013 (“TESEO” – PON02_00153-2939517 and “Plastic electronics for smart disposable systems” – PON02_00355- 3416798). AF thanks KAU for financial support.

Notes and references

^a Dipartimento di Fisica e Chimica, Università di Palermo, V.le delle Scienze ed. 17, 90128, Palermo, Italy Fax: 0039-590015; Tel: 0039-09123897983;

^b Istituto per lo Studio dei Materiali Nanostrutturati (ISMN), Consiglio Nazionale delle Ricerche (CNR), via Ugo La Malfa, 153, 90146 Palermo, Italy;

^c Polyera Corporation, 8045 Lamon Avenue, Skokie, IL 60077 (USA).

^d Department of Materials Science and Nanotechnology Engineering, Abdullah Gül University, Kayseri, Turkey.

^e Center of Excellence for Advanced Materials Research, King Abdulaziz University, Jeddah 21589, Saudi Arabia.

*Correspondence to: bruno.pignataro@unipa.it; afacchetti@polyera.com
Electronic Supplementary Information (ESI) available: synthesis of symmetric NDI systems and characterization; oxidation of NDI2ODT4 and EDOT; cyclic voltammetry during electropolymerization; polymerization kinetics; DFT calculations; optical band gaps; thin film morphology and solvent effects; XPS of the solid supported thin films; electrical measurements; electrochromic properties of PNDI2ODT4 thin films; contact angle measurements; effect of the monomer reduction; effect of thermal annealing on Copol [2] morphology; references. See DOI: 10.1039/b000000x/

References

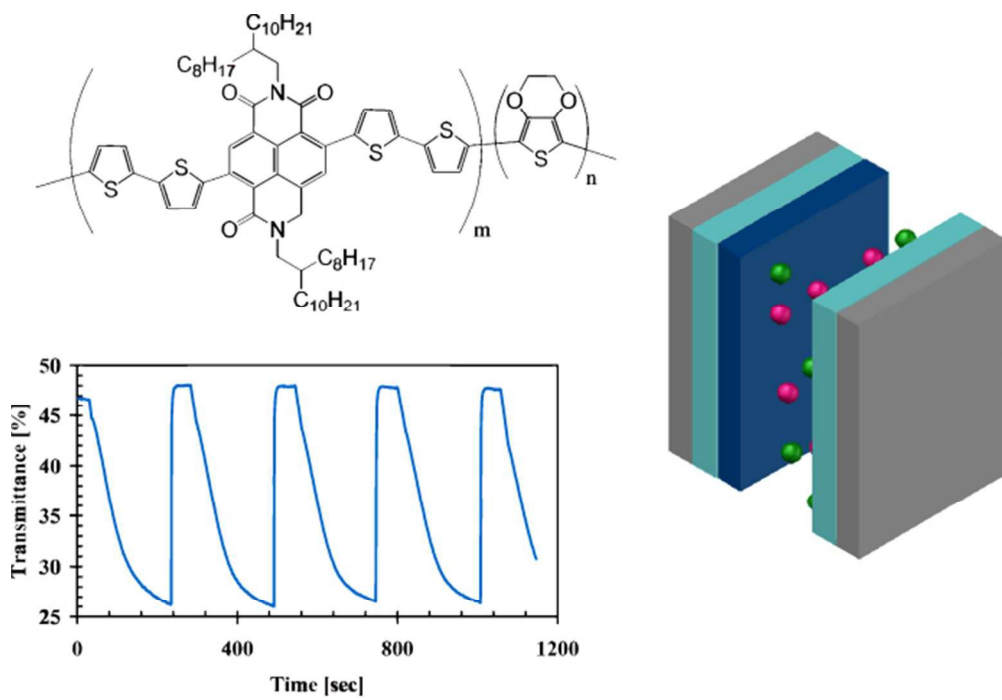
- 1 a) H. Sirringhaus, *Adv. Mater.*, 2005, 17, 2411. b) J. Smith, W. Zhang, R. Sougrat, K. Zhao, R. Li, D. Cha, A. Amassian, M. Heaney, I. McCulloch and T. D. Anthopoulos, *Adv. Mater.*, 2012, 24, 2441. 5 c) H. Chen, Y. Guo, G. Yu, Y. Zhao, J. Zhang, D. Gao, H. Liu and Y.

- Liu, *Adv. Mater.*, 2012, 24, 4618. *d*) Z. He, C. Zhong, S. Su, M. Xu, H. Wu, Y. Cao, *Nat. Photonics*, 2012, 6, 593; R. Liu, S. B. Lee, *J. Am. Chem. Soc.*, 2008, 130, 2942; *f*) Bartollini, E.; Seri, M.; Tortorella, S.; Facchetti, A.; Marks, T. J.; Marrocchi, A.; Vaccaro, L. *RSC Adv.* 2013, 3, 9288. *g*) Marrocchi, A.; Lanari, D.; Facchetti, A.; Vaccaro, L. *En. Envir. Sci.* 2012, 5, 8457. *h*) Okamoto, K.; Zhang, J.; Housekeeper, J. B.; Marder, S. R.; Luscombe, C. K. *Macromolecules* 2013, 46(20), 8059. *i*) M. Shao, J. Keum, J. Chen, Y. He, W. Chen, J. F. Browning, J. Jakowski, B. G. Sumpter, I. N. Ivanov, Y. Z. Ma, C. M. Rouleau, S. C. Smith, D. B. Geohegan, K. Hong, K. Xiao, *Nature Communications*, 2014, 5, doi:10.1038/ncomms4180.
- 2 *a*) J. Roncali, *Macromol. Rapid. Commun.*, 2007, 28, 1761; *b*) P. M. Beaujuge, S. Ellinger, J. R. Reynolds, *Nature Materials* 2008, 7, 795; *c*) C. B. Nielsen, A. Angerhofer, K. A. Abboud, J. R. Reynolds, *J. Am. Chem. Soc.* 2008, 130, 9734.
 - 3 *a*) Y. Ie, T. Sakurai, S. Jinnai, M. Karakawa, K. Okunda, S. Mori, Y. Aso, *Chem. Comm.*, 2013, 49, 8386; *b*) I. V. Sazanovich, M. A. H. Alamiry, J. Best, R. D. Bennet, O. V. Bouganov, E. S. Davies, V. P. Grivin, A. J. H. M. Meijer, V. F. Plyusnin, K. L. Ronayne, A. H. Skelton, S. A. Tikhomirov, M. Towrie, J. A. Weinstein, *Inorg. Chem.*, 2008, 47 (22), 10432; *c*) L. J. Rozanski, E. Castaldelli, F. L. M. Sam, C. A. Mills, G. J. F. Demets, S. R. P. Silva, *J. Mater. Chem. C* 2013, 1, 3347; *d*) S. Fabiano, H. Wang, C. Piliego, C. Jaye, D. A. Fischer, Z. Chen, B. Pignataro, A. Facchetti, Y.L. Loo, M. A. Loi, *Adv. Funct. Mater.* 2011, 21, 4479.
 - 4 *a*) Y. Kim, J. Hong, J. H. Oh, C. Yang, *Chem. Mater.*, 2013, 25, 3251; *b*) H. Yan, Z. Chen, Y. Zheng, C. Newman, J. R. Quinn, F. Dötz, M. Kastler, A. Facchetti, *Nature*, 2009, 457, 679. *b*) A. Facchetti, *Chem. Mater.*, 2011, 23, 733.
 - 5 R. Kim, P. S. K. Amegadze, I. Kang, H. J. Yun, Y. Y. Noh, S. K. Kwon, Y. H. Kim, *Adv. Funct. Mater.*, 2013, 23, 5719.
 - 6 *a*) X. Guo, M. D. Watson, *Org Lett* 2008, 10, 5333. *b*) M. M. Durban, P. D. Kazarinoff, C. K. Luscombe, *Macromolecules*, 2010, 43, 6348. *c*) F. S. Kim, X. Guo, M. D. Watson, S. A. Jenekhe, *Advanced Materials* 2010, 22, 478. *d*) X. Guo, F. S. Kim, M. J. Seger, S. A. Jenekhe, M. D. Watson, *Chem. Mater.* 2012, 24, 1434. *e*) Yuan, M.; Durban, M. M.; Kazarinoff, P. D.; Zeigler, D. F.; Rice, A. H.; Segawa, Y.; Luscombe, C. K. *J. Polym. Sci. A* 2013, 51(19), 4061-4069. *f*) A. Luzio, D. Fazzi, D. Natali, E. Giussani, K.J. Baeg, Z. Chen, Y. Y. Noh, A. Facchetti, M. Caironi, *Adv. Funct. Mater.*, 2014, 24, 1151.
 - 7 S. Fabiano, Z. Chen, S. Vahedi, A. Facchetti, B. Pignataro, M. A. Loi, *J. Mater. Chem.*, 2011, 21, 5891.
 - 8 Kim, N.-K.; Khim, D.; Xu, Y.; Lee, S.-H.; Kang, M.; Kim, J.; Facchetti, A.; Noh, Y.-Y.; Kim, D.-Y. *ACS Appl. Mater. Interf* 2014, 6(12), 9614.
 - 9 *a*) H. Krüger, S. Janietz, D. Sainova, D. Dobreva, N. Koch, A. Vollmer, *Adv. Funct. Mater.*, 2007, 17, 3715; *b*) M. Greenman, A.J. Ben-Sasson, Z. Chen, A. Facchetti, N. Tessler, *Appl. Phys. Lett.* 2013, 103, 073502/1.
 - 10 R. Kim, P. S. K. Amegadze, I. Kang, H. J. Yun, Y. Y. Noh, S. K. Kwon, Y. H. Kim, *Adv. Funct. Mater.*, 2013, 23, 5719.
 - 11 J. Roncali, P. Blanchard, P. Frère, *J. Mater. Chem.*, 2005, 15, 1589.
 - 12 *a*) G. A. Sotzing, C. A. Thomas and J. R. Reynolds, *Macromolecules*, 1998, 31, 3750; *b*) C. A. Thomas and J. R. Reynolds, in *ACS Symposium Series 735*, ed. B.R. Hsieh and Y. Wei, ACS, Washington DC, 1998, 367; *c*) S. Akoudad and J. Roncali, *Chem. Commun.*, 1998, 2081.
 - 13 H. Meng, D. Tucker, S. Chaffins, Y. Chen, R. Helgeson, B. Dunn and F. Wudl, *Adv. Mater.*, 2003, 15, 147.
 - 14 *a*) M. Sassi, M. M. Salamone, R. Ruffo, C. M. Mari, G. A. Pagani, L. Beverina, *Adv. Mater.*, 2012, 24, 2004; *b*) J. Cai, L. Ma, H. Niu, P. Zhao, Y. Lian, W. Wang, *Electroch. Acta*, 2013, 112, 59; *c*) T. Yijie, C. Haifeng, Z. Zhaoyang, X. Xiaoqian, Z. Yongjiang, *J. Electroanal. Chem.*, 2013, 689, 142.
 - 15 *a*) G. A. Yiseen, *Int. J. Electrochem. Sci.*, 2014, 9, 2575; *b*) G. A. Sotzing, J. R. Reynolds, P. J. Steel, *Adv. Mater.*, 1991, 9, No. 10, 795.
 - 16 *a*) P. Leriche, P. Blanchard, P. Frère, E. Levillain, G. Mabon, J. Roncali, *Chem. Commun.*, 2006, 275; *b*) J. Roncali, P. Blanchard, P. Frère, *J. Mater. Chem.*, 2005, 15, 1589.
 - 17 R. Steyleuthner, M. Schubert, I. Howard, B. Klaumünzer, K. Schilling, Z. Chen, P. Sallfrank, F. Laquai, A. Facchetti, D. Neher, *J. Am. Chem. Soc.* 134, 2012, 18303.
 - 18 D. K. Seo, R. Hoffmann, *Theor. Chem., Acc.*, 1999, 102, 23.
 - 19 Gursel Sonmez and Hayal B. Sonmez, *J. Mater. Chem.*, 2006, 16, 2473.
 - 20 Y. Kim, J. Hong, J. H. Oh, C. Yang, *Chem. Mater.*, 2013, 25, 3251.
 - 21 Y. Wei, Q. Zhang, Y. Jiang, J. Yu, *Macromol. Chem. Phys.*, 2009, 210, 769.
 - 22 *a*) J. Xia, N. Masaki, M. Lira-Cantu, Y. Kim, K. Jiang, S. Yanagida, *J. Am. Chem. Soc.*, 2008, 130, 4, 1258; *b*) V. Castagnola, C. Bayon, E. Descamps, C. Bergaud, *Synth. Met.*, 2014, 189, 7.
 - 23 R. Steyleuthner, M. Schubert, F. Jaiser, J. C. Blakesley, Z. Chen, A. Facchetti, D. Neher, *Adv. Mater.* 2010, 22, 2799.
 - 24 T. Yi-Jie, C. Hai-Feng, Z. Wen-Wei, Z. Zhao-Yang, *J. Appl. Polym. Sci.* 2013, 636.
 - 25 S. Hsiao, P. Chang, H. Wang, Y. Kung, T. Lee, *Journal of Polymer Science, Part A: Polymer Chemistry*, 2014, 52, 825.
 - 26 J. Cai, L. Ma, H. Niu, P. Zhao, Y. Lian, W. Wang, *Electrochimica Acta*, 2013, 112, 59.
 - 27 P.M.S. Monk, R. J. Mortimer, D. R. Rosseinsky, *Electrochromism and Electrochromic devices*, Cambridge University Press 2007
 - 28 E.G. Tolstopyatova, N.A. Pogulaichenko, S.N. Eliseeva, V.V. Kondratiev, *Russian Journal of Electrochemistry*, 2009, 45,3, 252
 - 29 T. Yijie, C. Haifeng, Z. Zhaoyang, X. Xiaoqian, Z. Yongjiang, *J. Electroanal. Chem.*, 2013, 689, 142.
 - 30 T. Yanai, D. Tew, N. Handy *Chem. Phys. Lett.*, 2004, 393, 51.
 - 31 *a*) D. Jacquemin, V. Wathelet, E. A. Perpète, C. Adamo *J. Chem. Theor. Comput.*, 2009, 5, 2420; *b*) S. Kupfer, J. Guthmüller, L. González *J. Chem. Theor. Comput.*, 2013, 9, 543.
 - 32 M. J. G. Peach, A. J. Cohen, D. J. Tozer *Phys. Chem. Chem. Phys.*, 2006, 8, 4543.
 - 33 Gaussian 09, Revision C.01, M. J. Frisch, G. W. Trucks, H. B. Schlegel, G. E. Scuseria, M. A. Robb, J. R. Cheeseman, G. Scalmani, V. Barone, B. Mennucci, G. A. Petersson, H. Nakatsuji, M. Caricato, X. Li, H. P. Hratchian, A. F. Izmaylov, J. Bloino, G. Zheng, J. L. Sonnenberg, M. Hada, M. Ehara, K. Toyota, R. Fukuda, J. Hasegawa, M. Ishida, T. Nakajima, Y. Honda, O. Kitao, H. Nakai, T. Vreven, J. A. Montgomery, Jr., J. E. Peralta, F. Ogliaro, M. Bearpark, J. J. Heyd, E. Brothers, K. N. Kudin, V. N. Staroverov, R. Kobayashi, J. Normand, K. Raghavachari, A. Rendell, J. C. Burant, S. S. Iyengar, J.

- Tomasi, M. Cossi, N. Rega, J. M. Millam, M. Klene, J. E. Knox, J. B. Cross, V. Bakken, C. Adamo, J. Jaramillo, R. Gomperts, R. E. Stratmann, O. Yazyev, A. J. Austin, R. Cammi, C. Pomelli, J. W. Ochterski, R. L. Martin, K. Morokuma, V. G. Zakrzewski, G. A. Voth, P. Salvador, J. J. Dannenberg, S. Dapprich, A. D. Daniels, Ö. Farkas, J. B. Foresman, J. V. Ortiz, J. Cioslowski, and D. J. Fox, Gaussian, Inc., Wallingford CT, 2009.
- 34 a) Briggs, D. Surface analysis of polymers by XPS and static SIMS; Cambridge University Press: Cambridge, U.K.1998.
- 35 a) Shirley, D.A., Phys. Rev. B, 1972, 5, 4709; b) Sherwood P.M.A.: "Data Analysis in X-ray Photoelectron Spectroscopy" in: Practical Surface Analysis by Auger and X-ray Photoelectron Spectroscopy , Briggs D. & Seah M.P. (Eds.), 445-474, Wiley New York, 1983.
- 36 Wagner, C.D.; Davis, L.E., Zeller, M.V., Taylor, J.A.; Raymond, R.H.; Gale, L. H., Surf. Interf. Anal. 1981, 3, 211.
- 37 Wagner C.D., Davis L.E., Riggs W.M., Surf. Interf. Anal. 1980, 2, 53.
- 38 Heinze J., Frontana Uribe B.A., Ludwigs S., Chem. Rev. 2010, 110, 4724.

TOC Entry Sentence

Novel electropolymerized copolymers with controlled donor/acceptor ratio by symmetric naphthalenediimidequaterthiophene showed prominent physico-chemical properties and high coloration efficiency electrochromic devices



58x40mm (300 x 300 DPI)